

Numerical Study of the Electrical Properties of Insulating Thin Films Deposited on a Conductive Substrate

Surajit Kumar, and Rosario A. Gerhardt*

School of Materials Science and Engineering, Georgia Institute of Technology, Atlanta, USA

*Corresponding author: 771 Ferst Drive, N.W., Love Bldg., Room 263, Atlanta, GA 30332, USA

Email address: rosario.gerhardt@mse.gatech.edu

Abstract: Parametric finite element simulations were performed to study the effect of film thickness, and electrode size on the different impedance parameters for insulating thin films deposited on a conductive substrate. COMSOL Multiphysics[®] was used to solve the quasi-static form of Maxwell's electromagnetic equations in time harmonic mode. Several types of 2D models (linear and axisymmetric) were considered. The full model dealt with a configuration in which the impedance is measured between two electrodes deposited on top of the films. The simplified models consisted of a top and a bottom electrode, while ignoring the substrate. By comparing the full model and the simplified models, approximations and generalizations were made. It was found that for highly insulating films, even simplified models can provide accurate capacitance values. However, the edge effects on the capacitance are found to be significant as the film thickness is increased or the electrode contact size is decreased.

Keywords: impedance, spectroscopy, dielectric, thin film.

1. Introduction

Measurement of the dielectric properties of thin films and nanostructures is an important aspect of their characterization. AC measurements carried out as a function of frequency is one of the most common methods for studying dielectric thin films [1]. AC measurements are often referred to as impedance spectroscopy (IS) or dielectric measurements (DS) [2]. In recent years this method is being extended to the nanometer scale range. One of the techniques for this is nanoscale capacitance microscopy (NCM) [3]. In this method the capacitance between an atomic force microscope (AFM) tip and the deposited material on a conductive substrate is measured. But, to the best of our knowledge, there have been no

systematic studies on the effect of the film properties and substrate properties on electrical measurements at the nanoscale. One needs to understand how film thickness, electrode/contact size as well as properties of the surrounding medium affect the measured response. This work is the first of a multi-part study that addresses the role the different parameters play in determining the accuracy of the measurements. In this paper, the effect of varying film thickness and electrode size are evaluated for the case of highly insulating thin films deposited onto a conductive substrate. The effect of other film properties and measurement parameters will be reported elsewhere. Future plans include performing 3D simulations to estimate the stray capacitance and other effects when an AFM tip is used to make impedance measurements as a function of frequency.

Some different approaches to the simulation of the electrical response of materials have been found in the literature. A finite difference method to solve Laplace's equations using a conjugate gradient algorithm was demonstrated by Coverdale et al. [4]. A transmission line model was used to simulate the impedances of electroactive layers with non-uniform resistance and/or capacitance profiles by Ren and Pickup [5]. A fractal model for grain boundary regions of ceramic materials was developed for impedance spectroscopy analysis by Branković et al. [6]. Using actual grain topologies, the steady-state electrical transport behavior in polycrystalline materials was simulated by Anderson and Ling [7]. In this paper, we take a finite element approach to solve for the electric potential and then calculate the impedance and related quantities through post-processing.

2. COMSOL Multiphysics Simulation

Several types of 2D models (linear and axisymmetric) were considered. The 2D (full) model dealt with a configuration in which the

impedance is measured between two electrodes deposited on top of the films. Figure 1 shows a schematic of the cross sectional side view of the structure that was simulated for calculation of the impedance of a thin film. It shows three subdomains: (1) the film of thickness, t_{film} , and electrical conductivity, σ_{film} , (2) the substrate of thickness, $t_{substrate}$, and electrical conductivity, $\sigma_{substrate}$, and (3) air of thickness, t_{air} , and electrical conductivity, σ_{air} . The electrodes are shown to have a width or diameter of $d_{electrode}$. The electrode thickness is ignored in the actual simulation because of the highly conductive nature of the electrode material since this is not likely to affect the result in any significant way. Also, incorporating the electrode thickness into the model would result in a significant increase in the number of mesh elements, putting additional demands on the limited computational resources. The simplified models consisted of a top and a bottom electrode, while ignoring the substrate.

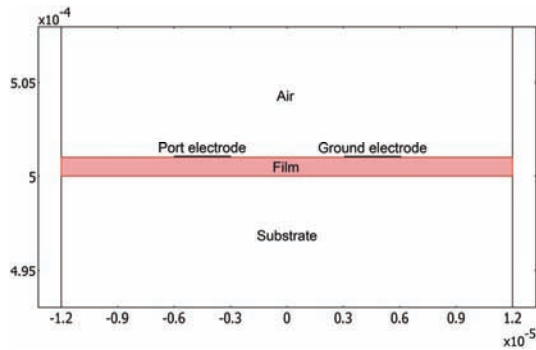


Figure 1. Schematic of a 2D (full) model for impedance/dielectric calculations for a thin dielectric film.

The numerical simulations were performed using the Time Harmonic-Electric Currents solver in the AC/DC Module of COMSOL Multiphysics® Version 3.4. The objective was to solve the quasi-static form of Maxwell's equations for the time harmonic electric potential phasor in 2D and 2D axisymmetric cases. For the computations, a dedicated Dell Precision T7400 workstation with eight Intel® Xeon® E5410 processors of 2.33 GHz speed, and a total of 8 GB RAM, running Windows XP

Professional x64 Edition, Version 2003, Service Pack 2, was used.

The electric field is simply the negative gradient of the electric potential. Dirichlet boundary conditions for the applied potentials were used on the electrodes, and Neumann boundary conditions were used for most other exterior boundaries, to model electrical insulation. Interior boundaries were generally modeled assuming continuity in the electric field displacements. The subdomains were meshed with a free mesh of unstructured triangular elements. Very fine mesh elements were defined near the electrodes, the thin film region, and the interfaces between the film and adjoining dielectric regions (air and substrate). Appropriate element sizes were selected for these small dimensions, and at locations near interfaces, where permittivity and conductivity changes were expected to be encountered. The maximum dimensions of the elements on the subdomain as a whole, and the edges of the interfaces were defined independently. The mesh elements were allowed to grow slowly into larger elements, as the distances increased away from the film interfaces.

In order to calculate the impedance, and capacitance, one of the electrodes was made a port, and the other electrode was made a ground (see Figure 1). The real and imaginary components of the lumped parameters of impedance (Z) or admittance (Y) at a particular port electrode were calculated by using the built in functions in COMSOL Multiphysics®. Capacitance (C) is then calculated from Z or Y . C , Z , and Y are complex quantities, and they can be expressed as $Z = 1/Y = Z' - jZ''$, $Y = 1/Z = Y' + jY''$, and $C = C' + jC'' = (Y'' + jY')/\omega$, where the real parts are indicated by single primes and the imaginary parts are indicated by double primes. There are three different choices of ports and hence, three different ways of calculating the lumped parameters: forced voltage, fixed current, and fixed current density. All the three methods were used and the results were compared to find out if they provided the same values.

Although the simulations could have been performed for arbitrary values of the dielectric

constants of the film and substrate, they were chosen as that of SiO₂ and highly doped Si, respectively since experiments were conducted using SiO₂ thin films grown on highly doped Si wafers. Standard permittivity values of air ($\epsilon_{air} = 1.00059 \epsilon_0$), SiO₂ ($\epsilon_{film} = 3.9 \epsilon_0$), and Si ($\epsilon_{substrate} = 11 \epsilon_0$) were used in the simulations, where $\epsilon_0 = 8.854 \times 10^{-12}$ F/m is the permittivity of vacuum. The conductivity of air was taken as $\sigma_{air} = 10^{-14}$ S/m while the conductivity of the substrate was chosen to be 100 S/m. The film conductivity used in the simulations was $\sigma_{film} = 10^{-13}$ S/m, which corresponds to the typical electrical conductivity of SiO₂. It was assumed that the film and the substrates are homogeneous and have uniform dielectric properties.

3. Results

3.1 Solver and Port Type Selection

During the initial simulations, a direct solver in COMSOL Multiphysics® called UMFPAK [8] was used for solving the potential field in the different subdomains of the model. Calculations were performed using the following parameters: $t_{air} \sim 500 \mu\text{m}$, $t_{film} = 100 \text{ nm}$, $t_{substrate} = 500 \mu\text{m}$, and $d_{electrode} = 3 \mu\text{m}$. It was found that this method provided unrealistic and incorrect results for the real part of impedance (Z') for any of the three types of port conditions applied on one of the electrodes in the model. The main concern was that the real part of impedance (Z') was indicated to have a negative value. This implies a negative resistance which is not realistic in normal circumstances for an insulating film. This is probably due to some numerical instability as a result of the high conductivity contrast between the film and the substrate. Following this revelation about the instabilities of the direct solvers, an iterative solver in COMSOL Multiphysics®, known as GMRES [9], was used for the simulations. The advantage of the iterative solver is that it requires less memory and can handle a much larger number of elements in a model. The downside is that the iterative solvers take a longer time to solve and convergence is not guaranteed for all conditions, often requiring adjustments in the mesh size and other parameters. However, since the iterative

solver provided the correct impedance values, it was used in all the simulations reported in this work.

Using the GMRES iterative solver, the three different port conditions (forced voltage, fixed current, and fixed current density) were tested using the same initial simulation parameters as before. It was found that all the methods provided essentially the same result. Hence, for the rest of the simulations, a port with forced voltage was used for the calculations. In this method, admittance (Y) is calculated using a built in function. Impedance (Z) and capacitance (C) are then obtained by post processing the calculated Y data.

3.2 Model Verification

To check if the COMSOL simulations provided correct quantitative values, a simulation was performed for the case of a simple parallel plate capacitor for a 1000 nm thick ($t_{film} = 1000 \text{ nm}$) film located between two parallel 3 μm size electrodes. The film was assumed to have a conductivity of $\sigma_{film} = 10^{-13}$ S/m. The simulations provided a value of the real part of capacitance which is almost exactly equal to the values obtained using the simple formula for a parallel plate capacitor [10]. This exercise showed that the numerical simulation procedure of mesh element selection and setup of the model, etc., were correct and that the results were consistent with the theoretically expected values.

Furthermore, the impedance and capacitance values were also calculated using ZView® software [11] and the material and measurement parameters used in the finite element simulations. Good agreement was found between the values obtained from the numerical simulations and the electrical circuit simulations as a function of frequency.

3.3 Effect of Film Thickness with Constant Conductivity

To study the effect of film thickness on the impedance quantities, simulations for the 2D (full) model were performed for different film thicknesses keeping the film conductivity a

constant. Figure 2(a) shows one of the resulting Bode plots of $-Z''$ as a function of frequency for several different film thicknesses. The color plot in Figure 2(b) shows the electric potential and field lines for a simulated 1000 nm thick SiO_2 film. For these insulating films, the Bode plots showed mostly linear variations for the real (Z') and imaginary ($-Z''$) components of impedance with frequency. The real component of capacitance (C') was found to be mostly frequency independent. The imaginary component of capacitance (C'') was also frequency independent, except for the presence of slight curvatures at the very low frequencies.

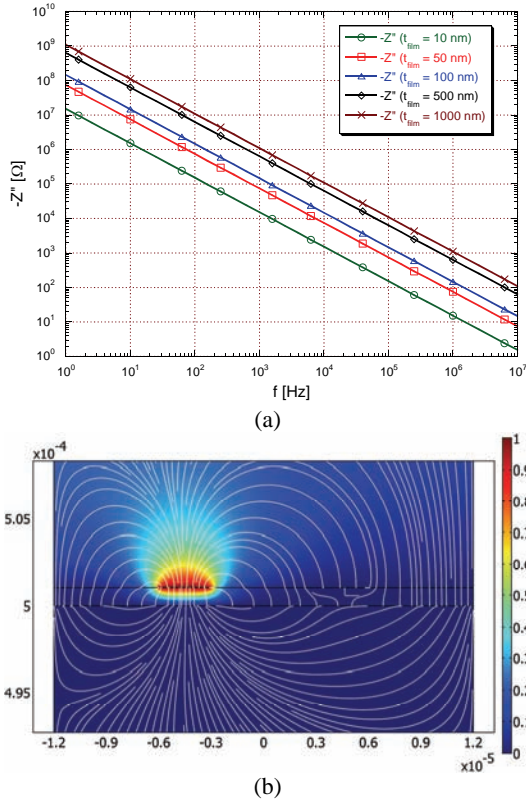


Figure 2. (a) Bode plots for 2D (full) model showing $-Z''$ for several film thicknesses, and (b) image showing the electric potential and field lines (white) for $t_{\text{film}} = 1000$ nm at 1 Hz frequency. The other simulation parameters are $d_{\text{electrode}} = 3 \mu\text{m}$; $t_{\text{air}} \sim 500 \mu\text{m}$, $\sigma_{\text{air}} = 10^{-14}$ S/m; $\sigma_{\text{film}} = 10^{-13}$ S/m; $t_{\text{substrate}} = 500 \mu\text{m}$, $\sigma_{\text{substrate}} = 100$ S/m.

3.4 Model Simplification for Films with Low Conductivity

To find out if the substrate had any effect on the impedance measurements, a simplified case of the model was simulated. Instead of two electrode pads on the same level on the top surface of the film, one pad was placed on the top of the film, and the whole bottom surface of the film was made the ground. This effectively ignored the highly conductive substrate below the film. Simulations were performed for different film thicknesses, while keeping the film conductivity, $\sigma_{\text{film}} = 10^{-13}$ S/m, a constant. The results showed that the $-Z''$ and C' characteristics are similar to the ones found in the case of the 2D (full) model. However, the Z' , and C'' characteristics showed the absence of curvatures in the very low frequencies.

3.5 Model Comparison

Figure 3 shows the comparison of the real part of capacitance (C') values calculated for a highly insulating film ($\sigma_{\text{film}} = 10^{-13}$ S/m) with the 2D (full) model, the 2D (simplified) model, and the parallel plate capacitor formula. The other simulation parameters used were the same as indicated in Figure 2.

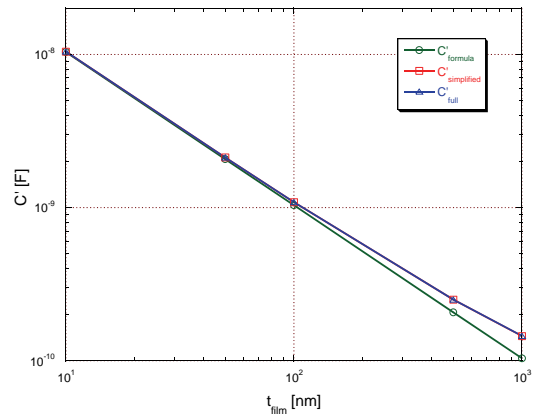


Figure 3. C' calculated using different methods plotted as a function of film thickness.

The $C'_{\text{simplified}}$ and C'_{full} values used in the plot are representative values from the flat portion of the C' versus frequency characteristics obtained from the simulations.

The $C'_{formula}$ values were calculated using the parallel plate capacitance formula [10]. It can be observed from the plot that the capacitance (C') for the 2D (full) model, and the 2D (simplified) model are almost equal. For the thinner films, this difference is negligible, while some difference can be seen for thicker films. This is expected and is due to edge effects [12].

3.6 Axisymmetric Models

Simple 2D axisymmetric models were simulated for three different circular electrode sizes: $d_{electrode} = 3, 30, \text{ and } 300 \mu\text{m}$, while keeping all the other parameters the same as in the full and simplified 2D models ($t_{air} \sim 500 \mu\text{m}$, $\sigma_{air} = 10^{-14} \text{ S/m}$; $t_{film} = 100 \text{ nm}$, $\sigma_{film} = 10^{-13} \text{ S/m}$). The calculations were performed using a top port electrode on the surface of the film, while the bottom of the film was made a ground. The substrate is not taken into consideration in this case because of its high conductivity and in light of the approximations discussed in the previous section. The pads are circular in this model as opposed to the 2D models described in the earlier sections. The calculated capacitances were again compared to the simple parallel plate capacitor model. The simulated values used for comparison are representative values from the flat portion of the C' curves. The difference is found to be significant only for the smallest electrode size, where edge effects are dominant [12] because the electrode diameter to film thickness ratio is less than 10.

4. Conclusions

Several 2D and 2D axisymmetric models were used to carry out parametric studies to find out the dependence of impedance and capacitance on film thickness, and electrode size as a function of frequency. The full and simplified models showed very little error when the films are very insulating and the substrate is highly conductive, as long as edge effects did not become significant. The edge effects on the capacitance are found to be significant as the film thickness is increased or the electrode contact size is decreased.

5. Acknowledgements

The authors would like to acknowledge the United States Department of Energy (DOE) for providing funding for this work under contract number DE-FG02-03-ER46035.

6. References

1. R. A. Gerhardt, "Impedance spectroscopy and mobility spectra", in *Encyclopedia of Condensed Matter Physics*, Academic Press, San Diego, CA, pp. 350-363 (2005)
2. E. Barsoukov (ed), and J. R. Macdonald (ed), *Impedance Spectroscopy: Theory, Experiment, and Applications*, 2nd Edition, Wiley-Interscience, New York (2005)
3. D. T. Lee, J. P. Pelz, and B. Bhushan, "Instrumentation for direct, low frequency scanning capacitance microscopy, and analysis of position dependent stray capacitance", *Review of Scientific Instruments*, **73**, 3525-3533 (2002)
4. R. T. Coverdale, H. M. Jennings, and E. Garboczi, "An improved model for simulating impedance spectroscopy", *Computational Materials Science*, **3**, 465-474 (1995)
5. X. Ren, and P. G. Pickup, "Simulation and analysis of the impedance behaviour of electroactive layers with non-uniform conductivity and capacitance profiles", *Electrochimica Acta*, **46**, 4177-4183 (2001)
6. G. Branković, Z. Branković, V. D. Jović, and J. A. Varela, "Fractal approach to AC impedance spectroscopy studies of ceramic materials", *Journal of Electroceramics*, **7**, 89-94 (2001)
7. M. P. Anderson, and S. Ling, "Computer simulation of transport in thin films", *Journal of Electronic Materials*, **19**, 1161-1169 (1990)
8. T.A. Davis, "Algorithm 832: UMFPACK V4.3 – an unsymmetric-pattern multifrontal method," *ACM Transactions on Mathematical Software*, **30**, 196-199 (2004)
9. Y. Saad and M.H. Schultz, "GMRES: A generalized minimal residual algorithm for solving nonsymmetric linear systems," *SIAM Journal on Scientific Computing*, **7**, 856-869 (1986)
10. D. J. Griffiths, *Introduction to Electrodynamics*, 3rd Edition, Prentice Hall (2003)
11. ZView[®] Software, Scribner and Associates, Inc. Southern Pines, NC
12. *ASTM D150-98 (2004) Standard Test Methods for AC Loss Characteristics and Permittivity (Dielectric Constant) of Solid Electrical Insulation*, ASTM International, West Conshohocken, PA (2004)